Bioorganic & Medicinal Chemistry 18 (2010) 7948–7956

Contents lists available at ScienceDirect

Bioorganic & Medicinal Chemistry

journal homepage: www.elsevier.com/locate/bmc

Design, syntheses and 3D-QSAR studies of novel *N*-phenyl pyrrolidin-2-ones and *N*-phenyl-1*H*-pyrrol-2-ones as protoporphyrinogen oxidase inhibitors

Li Zhang [a], Yin Tan [a], Neng-Xue Wang [a], Qiong-You Wu [a], Zhen Xi [b,*], Guang-Fu Yang [a,*]

[a] Key Laboratory of Pesticide & Chemical Biology, Ministry of Education, College of Chemistry, Central China Normal University, Wuhan 430079, PR China
[b] State Key Laboratory of Elemento-Organic Chemistry, Nankai University, Tianjin 300071, PR China

ARTICLE INFO

Article history:
Received 3 August 2010
Revised 14 September 2010
Accepted 15 September 2010
Available online 19 September 2010

Keywords:
Protoporphyrinogen oxidase
Herbicide
N-Phenyl pyrrolidin-2-one
N-Phenyl-*1H*-pyrrol-2-one
CoMFA

ABSTRACT

The characteristics of low application rates, good crop selectivity, low residue and environmental safety exhibited by Protoporphyrinogen oxidase (PPO, EC 1.3.3.4)-inhibiting herbicides have attracted a world-wide research interests. As continuation of our research work on the development of new PPO inhibitors, a series of mono-carbonyl analogues of cyclic imides, *N*-phenyl pyrrolidin-2-ones and *N*-phenyl-1*H*-pyrrol-2-ones, were designed and synthesized based on previously established DFT-QSAR results. The PPO inhibition activities of 29 newly synthesized compounds were tested and a predictive comparative molecular field analysis (CoMFA) model was established with the conventional correlation coefficient $r^2 = 0.980$ and the cross-validated coefficient $q^2 = 0.518$. According to the CoMFA model, the substituent effects on the PPO inhibition activity were explained reasonably. Further greenhouse assay showed that 2-(4-chloro-2-fluoro-5-propoxy-phenyl)-2,3,4,5,6,7-hexahydro-isoindol-1-one (**C**$_6$, $k_i = 0.095$ μM) and 2-(5-allyloxy-4-chloro-2-fluorophenyl)-2,3,4,5,6,7-hexahydro-isoindol-1-one (**C**$_7$, $k_i = 0.12$ μM) displayed excellent post-emergency herbicidal activity at the concentration of 150 g.ai/ha against seven tested weeds. Due to their high PPO inhibition effect and broad spectrum herbicidal activity, these two compounds have the potential for further study on crop selectivity and field trial. These results confirmed once again that only one of the carbonyl groups of cyclic imides is essential to the PPO inhibition activity.

1. Introduction

Protoporphyrinogen IX oxidase (PPO; EC 1.3.3.4), the last common enzyme in the biosynthetic pathway leading to heme and chlorophyll, has been identified as one of the most important action targets for chemically diverse herbicides such as diphenylethers,[1] phenylpyrazoles,[2] oxadiazoles,[3] triazolinones,[4] thiadiazoles,[5] pyrimidineones,[6] oxazolidinediones,[7] isoxazoles,[8] and *N*-phenyl phthalimides[9] that have been introduced into market for many years. The attributes of low application rates, good crop selectivity, low residue and environmental safety exhibited by these compounds are important characteristics for green agrochemicals. Therefore, PPO-inhibiting herbicides have achieved great success in agriculture market and attracted a world-wide research commitment.

Since 1990s, research on PPO inhibitors has been actively pursued, leading to two classes of commercial products, diphenyl ethers and *N*-phenyl phthalimides, especially the latter which has become a very interesting and hot research area.[9–12] Structural optimization of the pioneering compounds of *N*-phenyl phthalimides family (such as chlorphthalim) has led to discovery of some commercialized products, such as oxadiargyl, oxadiazon, sulfentrazone, and pentoxazone as shown Figure 1. As well known, *N*-phenyl phthalimides herbicides have a common structural feature of *N*-2,4,5-trisubstituted phenylnitrogen. The substituents patterns of phenyl group have been extensively investigated, but the role of two carboxyl group in the PPO-inhibiting activity attracted little attention.

Previously, we studied the quantitative structure–activity relationships of a series of cyclic imides (e.g., *N*-phenyl-1*H*-isoindole-1,3(2*H*)-dione, **A**) with various heterocyclic rings and substituents using the quantum chemical descriptors calculated at the B3LYP/6-31G(d,p) level.[13] Our DFT-QSAR results indicated that the approximate nucleophilic superdelocalizability of the carbon atom of one of the carbonyl group played an important role in determining the activity of PPO inhibitors. The stronger the ability of the carbonyl group to accept electrons from receptor, the higher the activity of PPO inhibitor. These results indicated that only one of the carbonyl groups is essential for the activity. Therefore, as a continuation of our research work on the development of new PPO inhibitors,[14,15] we are very interested in design and syntheses of *N*-phenyl pyrrolidin-2-ones (**B**) and *N*-phenyl-1*H*-pyrrol-2-ones (**C** and **D**) and as shown in Figure 2. As a control, three *N*-phenyl-1*H*-isoindole-1,3(2*H*)-diones (**A**) were also synthesized. In the present work,

* Corresponding authors. Tel.: +86 27 67867800; fax: +86 27 67867141 (G.-F.Y.).
E-mail addresses: gfyang@mail.ccnu.edu.cn, gfyang2010@yahoo.cn (G.-F. Yang).

0968-0896/$ - see front matter © 2010 Elsevier Ltd. All rights reserved.
doi:10.1016/j.bmc.2010.09.036

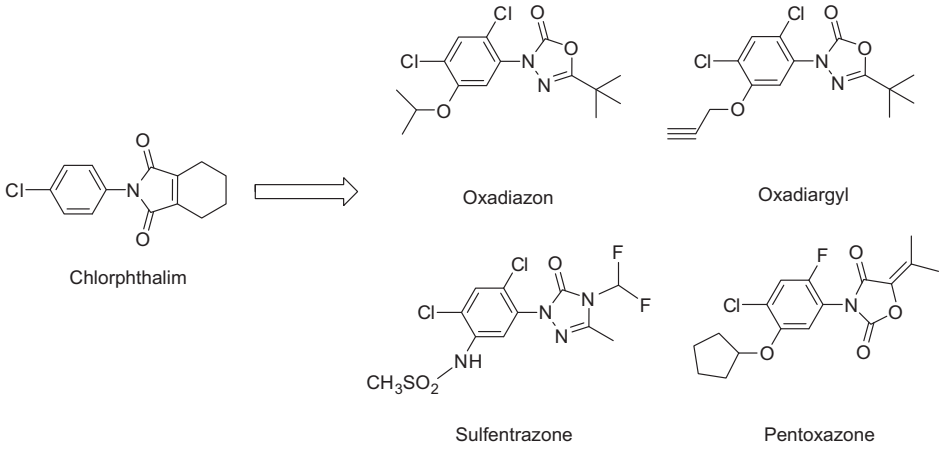

Figure 1. Structures of some commercial PPO inhibitors derived from chlorphthalim.

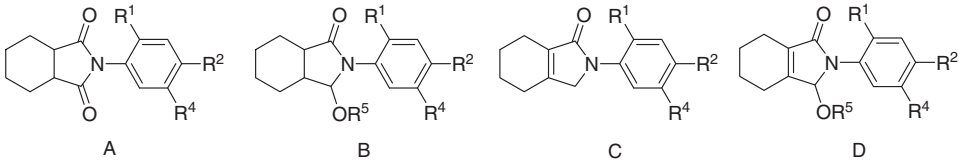

Figure 2. Structures of the designed compounds (**B**–**D**) and the control (**A**).

we report the detailed synthetic route, PPO-inhibiting activity and herbicidal activities of series **A**–**D**. The obtained result indicated that these compounds displayed good or excellent PPO inhibition activity and promising herbicidal activity. In addition, the three-dimensional quantitative structure–activity relationships of 29 newly synthesized compounds were also performed by using the method of Comparative Molecular Field Analysis (CoMFA).

2. Materials and methods

Unless otherwise noted, reagents were purchased from commercial suppliers and used without further purification, as all solvents were redistilled before use. ^{1}H NMR spectra were recorded on a Mercury-Plus 400 spectrometer (Variant Co., America) and samples were dissolved in $CDCl_3$ or DMSO with TMS as the internal reference. MS spectra were determined using a TraceMS 2000 organic mass spectrometer (Finnigan Co., America) and signals were recorded in *m*/*z*. Elemental analyses were performed on a Vario EL III elemental analysis instrument (Elementar Co., Germany). Melting points were measured on a Buchi B-545 melting point apparatus and are uncorrected. The starting material $\mathbf{M}_1$ and $\mathbf{M}_2$ were prepared according to the existing methods,[16,17] the intermediate $\mathbf{M}_3$ was prepared by applying the same procedure as the synthesis of compound **A**. The inhibition activity (k_i) of all target compounds against human PPO was tested as described previously,[14] 4-chlorophthalimide and sulfentrazone were selected as control. In Table 1, pk_i is the negative logarithm of k_i value.

2.1. General procedure for the synthesis of compound A_{1-3}

A mixture of intermediate $\mathbf{M}_1$ (5 mmol), anhydrous K_2CO_3 (7.5 mmol) in anhydrous *N*,*N*-dimethylformamide (DMF) was stirred for 0.5 h at room temperature and R^3X (10 mmol) was added. The resulted solution was stirred at room temperature until the reaction was completed according to the TLC detection. The reaction solution was poured into water. The product was extracted with ethyl acetate. The ethyl acetate phase was dried with $MgSO_4$ and evaporated at reduced pressure to obtain crude product, which was purified by column chromatography eluting with acetone/petroleum.

2.1.1. Data for A_1

Yield, 75%; white solid; mp 118–120 °C. ^{1}H NMR (400 MHz, $CDCl_3$): δ = 1.52–1.54 (m, 4H, 2 × $CHCH_2CH_2$–), 1.81–1.94 (m, 4H, 2 × $CHCH_2$–), 3.07–3.09 (m, 2H, 2 × COCH–), 3.88 (s, 3H, OCH_3), 6.73 (d, *J* = 6.0 Hz, 1H, –C(F) = CH), 7.28 (d, *J* = 8.8 Hz, 1H, NC═CH); EI-MS: *m*/*z* (%) 313 ([M+1]$^+$, 19), 312 (M$^+$, 17), 311 ([M−1]$^+$, 100), 201 (80), 81 (46), 67 (51). Anal. Calcd for $C_{15}H_{15}ClFNO_3$: C, 57.79; H, 4.85; N, 4.49. Found: C, 57.81; H, 4.45; N, 4.39.

2.1.2. Data for A_2

Yield, 85%; yellow oil; ^{1}H NMR (400 MHz, $CDCl_3$): δ = 1.31–1.32 (m, 3H, $-CH_2CH_3$), 1.45–1.58 (m, 4H, 2 × $CHCH_2CH_2$–), 1.82–1.95 (m, 4H, 2 × $CHCH_2$–), 3.07–3.09 (m, 2H, 2 × COCH–), 4.28–4.32 (m, 2H, $-CH_2CH_3$), 4.68 (s, 2H, $-OCH_2$–), 6.76 (d, *J* = 6.4 Hz, 1H, –C(F)═CH), 7.30 (d, *J* = 8.8 Hz, 1H, NC═CH); EI-MS: *m*/*z* (%) 385 ([M+1]$^+$, 28), 384 (M$^+$, 25), 383 ([M−1]$^+$, 60), 301 (62), 116 (97), 115 (61), 88 (52), 81 (71), 66(100), 60 (54), 57 (55), 54 (68), 45 (58), 41 (80). Anal. Calcd for $C_{18}H_{19}ClFNO_5$: C, 56.33; H, 4.99; N, 3.65; Found: C, 56.07; H, 4.78; N, 3.19.

2.1.3. Data for A_3

Yield, 88%; yellow oil; ^{1}H NMR (400 MHz, $CDCl_3$): δ = 1.27–1.28 (m, 3H, $-CH_2CH_3$), 1.51–1.52 (m, 4H, 2 × $CHCH_2CH_2$–), 1.67 (d, *J* = 6.4 Hz, 3H, $CHCH_3$), 1.85–1.95 (m, 4H, 2 × $CHCH_2$–), 3.06–3.08 (m, 2H, 2 × COCH–), 4.19–4.24 (m, 2H, $-CH_2CH_3$), 4.70 (q, *J* = 6.8 Hz, 1H, CH), 6.77 (d, *J* = 6.4 Hz, 1H, –C (F)═CH), 7.30 (d, *J* = 9.2 Hz, 1H, NC═CH); EI-MS: *m*/*z* (%) 399 ([M+1]$^+$, 28), 398 (M$^+$, 0), 397 ([M−1]$^+$, 98), 324 (97), 297 (88), 187 (55), 104 (90), 77 (72), 72 (100), 43 (91). Anal. Calcd for $C_{19}H_{21}ClFNO_5$: C, 57.36; H, 5.32; N, 3.52. Found: C, 57.07; H, 5.22; N, 3.37.

Table 1
Structures and PPO-inhibiting activities of the title compounds

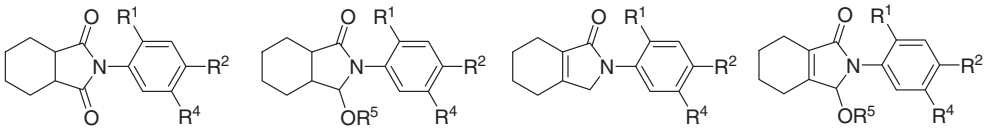

Training set							
No.	R^1	R^2	R^4	R^5	k_i (μM)	$pk_{i(exp)}$	$pk_{i(cal)}$
A_1	F	Cl	OCH_3	/	8.22	5.09	4.87
A_2	F	Cl	$OCH_2CO_2C_2H_5$	/	15.24	4.82	5.07
A_3	F	Cl	$OCH(CH_3)CO_2C_2H_5$	/	3.30	5.48	5.29
B_1	F	Cl		H	24.64	4.61	4.58
B_3	F	Cl	OCH_3	H	130.97	3.88	4.07
B_4	F	Cl	$OCH_2CO_2C_2H_5$	H	123.78	3.91	4.07
B_5	F	Cl	$OCH(CH_3)CO_2C_2H_5$	H	48.07	4.32	4.31
B_6	F	Cl	OCH_2CCH	H	63.63	4.20	4.16
B_7	F	Cl	OCH_2CHCH_2	H	44.83	4.34	4.37
C_1	F	Cl	$OCH(CH_3)_2$	—	0.69	6.16	6.04
C_2	H	Cl	NH_2	—	27.64	4.56	4.51
C_4	F	Cl	OCH_2CH_3	—	0.20	6.70	6.80
C_5	Cl	Cl	$OCH_2CH_2CH_3$	—	0.30	6.52	6.60
C_6	F	Cl	$OCH_2CH_2CH_3$	—	0.095	7.02	7.01
C_7	F	Cl	OCH_2CHCH_2	—	0.12	6.92	6.85
D_1	F	Br	OH	H	19.35	4.71	4.67
D_2	F	Cl	3-F–$C_6H_4CH_2O$	H	0.78	6.11	6.19
D_4	Cl	Cl	OCH_2CHCH_2	H	7.45	5.13	5.41
D_5	F	Cl	OCH_2CHCH_2	H	1.03	5.99	6.04
D_6	OCH_2CH_3	Cl	NO_2	H	358.6	3.45	3.42
D_7	F	Br	OH	CH_2CHCH_2	41.35	4.38	4.21
D_8	F	Cl	3-Cl–$C_6H_4CH_2O$	CH_3	1.03	5.99	5.63
D_9	F	Cl	OCH_3	CH_3	4.49	5.35	5.42
D_{10}	F	Cl	3-Cl–$C_6H_4CH_2O$	CH_2CHCH_2	66.58	4.18	4.24
Test set							
B_2	F	Cl	$OCH(CH_3)_2$	H	47.35	4.32	4.09
C_3	Cl	Cl	OCH_2CH_3	—	0.67	6.17	6.21
D_3	F	Cl	3-Cl–$C_6H_4CH_2O$	H	0.53	6.28	6.21
D_{11}	F	Cl	OCH_2CHCH_2	CH_2CHCH_2	33.13	4.48	4.11
D_{12}	F	Cl	OCH_2CH_3	CH_2CHCH_2	7.02	5.15	5.89
4-Chloro-phthalimide					87.87	4.06	/
Sulfentrazone					0.72	6.14	/

2.2. General procedure for the synthesis of compound B_{1-7}

A mixture of compound **A** (1 mmol) in anhydrous methanol was stirred at room temperature. $NaBH_4$ (1 mmol) was added portion wise and the mixture was stirred for about 2 h. The reaction solution was poured into ice water (30 mL). Precipitated solids were filtered and recrystallized from acetone or ethanol to give the pure title compounds.

2.2.1. Data for B_1

Yield, 95%; white solid; mp 157–158 °C. ^{1}H NMR (400 MHz, $CDCl_3$): δ = 1.21–1.64 (m, 8H, –OCHCH$_2$C*H*$_2$C*H*$_2$–; COCHCH$_2$-C*H*$_2$C*H*$_2$–), 1.81–1.96 (m, 8H, 2 × CHC*H*$_2$–; 2 × OCHC*H*$_2$–), 2.14–2.19 (m, 1H, COCH), 2.34–2.38 (m, 1H, C (OH) C*H*), 4.72–4.76 (m, 1H, OCH), 5.10 (s, 1H, –(OH)C*H*), 7.02 (d, J = 7.2 Hz, 1H, –C(F)═CH), 7.18 (d, J = 6.0 Hz, 1H, NC═CH); EI-MS: m/z (%) 369 ([M+1]$^+$, 22), 368 (M$^+$, 12), 367 ([M−1]$^+$, 61), 301 (62), 299 (95), 281 (55), 189 (88), 187 (87), 161 (100), 93 (62), 41 (70). Anal. Calcd for $C_{19}H_{23}ClFNO_3$: C, 62.04; H, 6.30; N, 3.81. Found: C, 62.02; H, 6.01; N, 3.70.

2.2.2. Data for B_2

Yield, 88%; white solid; mp 151–153 °C. ^{1}H NMR (400 MHz, $CDCl_3$): δ = 1.24–1.26 (m, 4H, 2 × CHC*H*$_2$–), 1.36–1.37 (m, 6H, 2 × CHC*H*$_3$), 1.37–1.39 (m, 4H, 2 × CHC*H*$_2$–), 2.62–2.68 (m, 1H, COCH), 2.98–3.00 (m, 1H, C(OH)C*H*), 4.46–4.50 (m, 1H, OCH), 5.12 (s, 1H, –(OH) C*H*), 7.05 (d, J = 6.8 Hz, 1H, –C(F)═CH), 7.22 (d, J = 10.0 Hz, 1H, NC═CH); EI-MS: m/z (%) 343 ([M+1]$^+$, 21), 342 (M$^+$, 39), 341 ([M−1]$^+$, 100), 323 (44), 299 (59), 161 (31). Anal. Calcd for $C_{17}H_{21}ClFNO_3$: C, 59.74; H, 6.19; N, 4.10. Found: C, 59.88; H, 6.08; N, 3.93.

2.2.3. Data for B_3

Yield, 68%; white solid; mp 139–140 °C. ^{1}H NMR (400 MHz, $CDCl_3$): δ = 1.23–2.18 (m, 8H, –CH$_2$CH$_2$CH$_2$CH$_2$–), 2.38–2.39 (m, 1H, COCH), 2.99–3.00 (m, 1H, –CH(OH)C*H*–), 3.88 (s, 3H, OCH_3), 5.11 (s, 1H, C*H*(OH), 7.01 (d, J = 6.8 Hz, 1H, –C(F)═CH), 7.43 (d, J = 6.4 Hz, 1H, NC═CH); EI-MS: m/z (%) 315 ([M+1]$^+$, 12), 314 (M$^+$, 21), 313 ([M−1]$^+$, 49), 176 (36), 175 (99), 174 (100), 81 (37). Anal. Calcd for $C_{15}H_{17}ClFNO_3$: C, 57.42; H, 5.46; N, 4.46. Found: C, 57.36; H, 5.23; N, 4.25.

2.2.4. Data for B_4

Yield, 70%; white solid; mp 154–156 °C. ^{1}H NMR (400 MHz, $CDCl_3$): δ = 1.24–1.28 (m, 3H, CH_2CH_3), 1.57–2.12 (m, 8H, $-CH_2CH_2CH_2CH_2-$), 2.34–2.39 (m, 1H, COCH), 2.96–2.98 (m, 1H, –CH(OH)*CH*–), 3.81 (s, 2H, OCH_2), 4.67–4.69 (m, 2H, CH_2CH_3), 5.09 (s, 1H, *CH*(OH), 7.01 (d, J = 4.4 Hz, 1H, –C(F)=CH), 7.43 (d, J = 10.4 Hz, 1H, NC=CH); EI-MS: m/z (%) 386 ($[M+1]^+$, 11), 385 (M^+, 17), 384 ($[M-1]^+$, 9), 370 (44), 261 (44), 259 (47), 233 (93), 231 (58), 93 (90), 90 (45), 81 (100), 67 (83), 66 (59), 57 (63), 54 (77), 41 (69). Anal. Calcd for $C_{18}H_{21}ClFNO_5$: C, 56.04; H, 5.49; N, 3.63. Found: C, 55.93; H, 5.12; N, 3.57.

2.2.5. Data for B_5

Yield, 68%; white solid; mp 105–107 °C. ^{1}H NMR (400 MHz, $CDCl_3$): δ = 1.19–1.29 (m, 6H, CH_2CH_3 and $CHCH_3$), 1.59–2.16 (m, 8H, $-CH_2CH_2CH_2CH_2-$), 2.35–2.37 (m, 1H, COCH), 2.96–2.98 (m, 1H, –CH(OH)*CH*–), 4.20–4.25 (m, 2H, $-CH_2CH_3$), 4.70–4.72 (m, 1H, O*CH*CH_3), 5.05 (s,1H, *CH* (OH), 7.02 (d, J = 6.8 Hz, 1H, –C(F)=CH), 7.43 (d, J = 10.0 Hz, 1H, NC=CH); EI-MS: m/z (%) 401 ($[M+1]^+$, 16), 399 ($[M-1]^+$, 52), 161 (89), 95 (48), 93 (100), 91 (48), 81 (78), 79 (50), 55 (50). Anal. Calcd for $C_{19}H_{23}ClFNO_5$: C, 57.07; H, 5.80; N, 3.50. Found: C, 56.90; H, 5.61; N, 3.24.

2.2.6. Data for B_6

Yield, 88%; white solid; mp 156–158 °C. ^{1}H NMR (400 MHz, $CDCl_3$): δ = 1.22–2.39 (m, 8H, $-CH_2CH_2CH_2CH_2-$), 2.58 (s, 1H, ≡CH), 2.69–2.72 (m, 1H, COCH), 2.98–3.00 (m, 1H, –CH(OH)*CH*–), 4.76 (s, 2H, $-OCH_2-$), 5.11 (s, 1H, *CH*(OH), 7.20–7.24 (m, 2H, ArH); EI-MS: m/z (%) 339 ($[M+1]^+$, 17), 338 (M^+, 27), 337 ($[M-1]^+$, 65), 94 (99), 79 (99), 66 (100), 60 (54), 53 (99). Anal. Calcd for $C_{17}H_{17}ClFNO_3$: C, 60.45; H, 5.07; N, 4.15. Found: C, 60.62; H, 4.89; N, 4.02.

2.2.7. Data for B_7

Yield, 90%; grey solid; mp 132–134 °C. ^{1}H NMR (400 MHz, $CDCl_3$): δ = 1.21–2.39 (m, 8H, $-CH_2CH_2CH_2CH_2-$), 2.68–2.71 (m, 1H, COCH), 2.98–3.00 (m, 1H, –CH(OH)*CH*–), 4.57 (d, J = 5.2 Hz, 2H, $-OCH_2-$), 5.11 (s, 1H, *CH*(OH), 5.31 (d, J = 10.8 Hz, 1H, CH=*CH*H), 5.44 (d, J = 10.8 Hz, 1H, CH=CH*H*), 6.01–6.05 (m, 1H, –*CH*=CH_2), 7.04–7.24 (m, 2H, ArH); EI-MS: m/z (%) 341 ($[M+1]^+$, 49), 340 (M^+, 46), 339 ($[M-1]^+$, 100), 95 (61), 93 (97), 81 (87), 67 (90), 55 (65). Anal. Calcd for $C_{17}H_{19}ClFNO_3$: C, 60.09; H, 5.64; N, 4.12. Found: C, 59.36; H, 5.29; N, 3.92.

2.3. General procedure for the synthesis of compound C_{1-7}

Compound **B** (1 mmol) was dissolved in anhydrous methanol (20 mL). The solution was acidified with concentrated hydrochloric acid until the pH of the mixture was set to be pH 1. The reaction mixture was stirred at room temperature for 14 h and concentrated in vacuo. Then, water (100 mL) was added and the product was extracted with dichloromethane. The dichloromethane phase was dried with magnesium sulfate and concentrated in vacuo. The obtained crude product was purified by column chromatography eluting with acetone/petroleum.

2.3.1. Data for C_1

Yield, 70%; white solid; mp 92–94 °C. ^{1}H NMR (400 MHz, $CDCl_3$): δ = 1.37 (d, J = 6.4 Hz, 6H, 2 × $CHCH_3$), 1.78–1.85 (m, 4H, $-CH_2CH_2CH_2CH_2-$), 2.28–2.35 (m, 4H, $-CH_2C{=}CCH_2-$), 4.30 (s, 2H, $-CH_2-$), 4.48–4.50 (m, 1H, OCH), 7.15 (d, J = 11.2 Hz, 1H, –C(F)=CH), 7.43 (d, J = 7.4 Hz, 1H, NC=CH); EI-MS: m/z (%) 324 (M^+, 2), 323 ($[M-1]^+$, 7), 90 (66), 77 (50), 42 (82), 41 (100). Anal. Calcd for $C_{17}H_{19}ClFNO_2$: C, 63.06; H, 5.91; N, 4.33. Found: C, 63.12; H, 5.80; N, 4.02.

2.3.2. Data for C_2

Yield, 85%; white solid; mp 102–104 °C. ^{1}H NMR (400 MHz, $CDCl_3$): δ = 1.75–1.80 (m, 4H, 5-CH_2, 6-CH_2), 2.28–2.34 (m, 4H, 4-CH_2, 7-CH_2), 4.19 (s, 2H, 3-CH_2), 6.75–6.98 (m, 3H, Ph). Anal. Calcd for $C_{14}H_{15}ClN_2O$: C, 64.00; H, 5.75; N, 10.66. Found: C, 64.50; H, 5.95; N, 10.65 .

2.3.3. Data for C_3

Yield, 75%; white solid; mp 89–90 °C. ^{1}H NMR (400 MHz, $CDCl_3$): δ = 1.45 (t, 3H, J = 6.8 Hz, OCH_2CH_3), 1.75–1.81 (m, 4H, 5-CH_2, 6-CH_2), 2.29–2.35 (m, 4H, 4-CH_2, 7-CH_2), 4.06 (q, 2H, J = 10.4 Hz, O*CH*$_2$CH$_3$), 4.22 (s, 2H, 3-CH_2), 6.92 (s, 1H, Ph), 7.45 (s, 1H, Ph). Anal. Calcd for $C_{16}H_{17}Cl_2NO_2$: C, 58.91; H, 5.25; N, 4.29. Found: C, 58.84; H, 5.14; N, 4.23.

2.3.4. Data for C_4

Yield, 74%; white solid; mp 90–92 °C. ^{1}H NMR (400 MHz, $CDCl_3$): δ = 1.45 (t, J = 6.8 Hz, 3H, OCH_2CH_3), 1.78–1.81 (m, 4H, 5-CH_2, 6-CH_2), 2.28–2.35 (m, 4H, 4-CH_2, 7-CH_2), 4.08 (q, J = 10.4 Hz, 2H, O*CH*$_2$CH$_3$), 4.30 (s, 2H, 3-CH_2), 7.16–7.43 (m, 2H, Ph). Anal. Calcd for $C_{16}H_{17}ClFNO_2$: C, 62.04; H, 5.53; N, 4.25. Found: C, 62.51; H, 5.64; N, 4.62.

2.3.5. Data for C_5

Yield, 72%; white solid; mp 76–78 °C. ^{1}H NMR (400 MHz, $CDCl_3$): δ = 1.04 (t, J = 7.4 Hz, 3H, $OCH_2CH_2CH_3$), 1.78–1.86 (m, 6H, $OCH_2CH_2CH_3$, 5-CH_2, 6-CH_2), 2.30–2.35 (m, 4H, 4-CH_2, 7-CH_2), 3.95 (t, J = 6.6 Hz, 2H, O*CH*$_2$CH$_2$CH$_3$), 4.23 (s, 2H, 3-CH_2), 6.91 (s, 1H, Ph) 7.45 (s, 1H, Ph). Anal. Calcd for $C_{17}H_{19}Cl_2NO_2$: C, 60.01; H, 5.63; N, 4.12. Found: C, 60.49; H, 5.25; N, 4.18.

2.3.6. Data for C_6

Yield, 76%; white solid; mp 80–81 °C. ^{1}H NMR (400 MHz, $CDCl_3$): δ = 1.04 (t, J = 7.6 Hz, 3H, $OCH_2CH_2CH_3$), 1.77–1.86 (m, 6H, $OCH_2CH_2CH_3$, 5-CH_2, 6-CH_2), 2.29–2.35 (m, 4H, 4-CH_2, 7-CH_2), 3.96 (t, J = 6.4 Hz, 2H, O*CH*$_2$CH$_2$CH$_3$), 4.30 (s, 2H, 3-CH_2), 7.15–7.41 (m, 2H, Ph). Anal. Calcd for $C_{17}H_{19}ClFNO_2$: C, 63.06; H, 5.91; N, 4.33. Found: C, 62.82; H, 5.61; N, 4.29.

2.3.7. Data for C_7

Yield, 71%; white solid; mp 112–114 °C. ^{1}H NMR (400 MHz, $CDCl_3$): δ = 1.75–1.80 (m, 4H, 5-CH_2, 6-CH_2), 2.29–2.35 (m, 4H, 4-CH_2, 7-CH_2), 4.31 (s, 2H, 3-CH_2), 4.58 (d, J = 2.4 Hz, 2H, O*CH*$_2$CHCH$_2$), 5.30–5.33 (m, 1H, OCH_2CHCH_2), 5.44–5.49 (m, 1H, OCH_2CHCH_2), 6.02–6.06 (m, 1H, OCH_2CHCH_2), 7.16–7.46 (m, 2H, Ph). Anal. Calcd for $C_{17}H_{17}ClFNO_2$: C, 63.46; H, 5.33; N, 4.35. Found: C, 63.54; H, 5.52; N, 4.34.

2.4. General procedure for the synthesis of compound D_{1-12}

A mixture of compound $\mathbf{M}_3$ (1 mmol) in anhydrous methanol was stirred at room temperature. $NaBH_4$ (1 mmol) was added portion wise and the mixture was stirred for about 2 h. The reaction solution was poured into ice water (30 mL). Precipitated solids were filtered and recrystallized from acetone or ethanol to give the pure compounds **D** with free hydroxyl group. Then, by applying the similar procedure as described for the synthesis of compound **A**, the alkylation of hydroxyl group afforded the corresponding hydroxyl-protected products **D**.

2.4.1. Data for D_1

Yield, 80%; white solid; mp 110–112 °C. ^{1}H NMR (400 MHz, $CDCl_3$): δ = 1.74–1.78 (m, 4H, 5-CH_2, 6-CH_2), 2.28–2.46 (m, 4H, 4-CH_2, 7-CH_2), 5.73 (s, 1H, CH), 7.35–7.40 (m, 3H, Ph). Anal. Calcd for $C_{14}H_{13}BrFNO_2$: C, 51.55; H, 4.02; N, 4.29. Found: C, 52.00; H, 4.19; N, 4.27.

2.4.2. Data for D_2

Yield, 72%; white solid; mp 102–103 °C. ^{1}H NMR (400 MHz, $CDCl_3$): δ = 1.73–1.82 (m, 4H, 5-CH_2, 6-CH_2), 2.27–2.50 (m, 4H, 4-CH_2, 7-CH_2), 5.08 (q, J = 9 Hz, 2H, OCH_2), 5.78 (s, 1H, CH), 7.03–7.37 (m, 6H, Ph). Anal. Calcd for $C_{21}H_{18}ClF_2NO_3$: C, 62.15; H, 4.47; N, 3.45. Found: C, 61.48; H, 5.03; N, 3.03.

2.4.3. Data for D_3

Yield, 78%; white solid; mp 115–116 °C. ^{1}H NMR (400 MHz, $CDCl_3$): δ = 1.72–1.78 (m, 4H, 5-CH_2, 6-CH_2), 2.27–2.53 (m, 4H, 4-CH_2, 7-CH_2), 5.06 (q, J = 8.2 Hz, 2H, OCH_2), 5.79 (s, 1H, CH), 7.23–7.46 (m, 6H, Ph). Anal. Calcd for $C_{21}H_{18}Cl_2FNO_3$: C, 59.73; H, 4.30; N, 3.32. Found: C, 59.80; H, 4.66; N, 3.17.

2.4.4. Data for D_4

Yield, 67%; white solid; mp 98–99 °C. ^{1}H NMR (400 MHz, $CDCl_3$): δ = 1.74–1.79 (m, 4H, 5-CH_2, 6-CH_2), 2.30–2.47 (m, 4H, 4-CH_2, 7-CH_2), 4.57–4.58 (m, 2H, OCH_2CHCH$_2$), 5.32–5.48 (m, 2H, OCH_2CHCH_2), 5.68 (s, 1H, CH), 6.01–6.08 (m, 1H, OCH_2CHCH_2), 6.89 (s, 1H, Ph), 7.50 (s, 1H, Ph). Anal. Calcd for $C_{17}H_{17}Cl_2NO_3$: C, 57.64; H, 4.84; N, 3.95. Found: C, 56.98; H, 5.13; N, 3.87.

2.4.5. Data for D_5

Yield, 72%; white solid; mp 102–103 °C. ^{1}H NMR (400 MHz, $CDCl_3$): δ = 1.70–1.85 (m, 4H, 5-CH_2, 6-CH_2), 2.26–2.45 (m, 4H, 4-CH_2, 7-CH_2), 4.56–4.58 (m, 2H, OCH_2CHCH$_2$), 5.31–5.48 (m, 2H, OCH_2CHCH_2), 5.78 (s, 1H), 6.01–6.08 (m, 1H, OCH_2CHCH_2), 7.16–7.23 (m, 2H, Ph); EI-Ms (m/z) 337 (M^+). Anal. Calcd for $C_{17}H_{17}ClFNO_3$: C, 60.45; H, 5.07; N, 4.15. Found: C, 60.38; H, 5.09; N, 3.77 .

2.4.6. Data for D_6

Yield, 78%; white solid; mp 114–115 °C. ^{1}H NMR (400 MHz, $CDCl_3$): δ = 1.45 (t, J = 7.0 Hz, 3H, OCH_2CH_3), 1.74–1.74 (m, 4H, 5-CH_2, 6-CH_2), 2.18–2.29 (m, 4H, 4-CH_2, 7-CH_2), 4.17 (q, J = 7.2 Hz, 2H, OCH_2CH_3), 5.78 (s, 1H, CH), 7.05 (s, 1H, Ph), 8.08 (s, 1H, Ph). Anal. Calcd for $C_{16}H_{17}ClN_2O_5$: C, 54.47; H, 4.86; N, 7.94. Found: C, 54.88; H, 4.56; N, 7.76.

2.4.7. Data for D_7

Yield, 73%; white solid; mp 112–113 °C. ^{1}H NMR (400 MHz, $CDCl_3$): δ = 1.73–1.83 (m, 4H, 5-CH_2, 6-CH_2), 2.31–2.34 (m, 4H, 4-CH_2, 7-CH_2), 3.71–3.85 (m, 2H, OCH_2CHCH$_2$), 5.10–5.19 (m, 2H, OCH_2CHCH_2), 5.70–5.77 (m, 1H, OCH_2CHCH_2), 5.80 (s, 1H, CH), 7.29–7.36 (m, 3H, Ph). Anal. Calcd for $C_{17}H_{17}BrFNO_2$: C, 55.75; H, 4.68; N, 3.82. Found: C, 55.47; H, 4.66; N, 3.75.

2.4.8. Data for D_8

Yield, 74%; white solid; mp 65–67 °C. ^{1}H NMR (400 MHz, $CDCl_3$): δ = 1.74–1.84 (m, 4H, 5-CH_2, 6-CH_2), 2.32 (s, 4H, 4-CH_2, 7-CH_2), 3.02 (s, 3H, OCH_3), 5.08 (q, J = 22.0 Hz, 2H, OCH_2), 5.78 (s, 1H, CH), 7.13–7.46 (m, 6H, Ph). Anal. Calcd for $C_{22}H_{20}Cl_2FNO_3$: C, 60.56; H, 4.62; N, 3.21. Found: C, 61.03; H, 4.84; N, 3.16.

2.4.9. Data for D_9

Yield, 84%; white solid; mp 124–125 °C. ^{1}H NMR (400 MHz, $CDCl_3$): δ = 1.74–1.86 (m, 4H, 5-CH_2, 6-CH_2), 2.31–2.32 (m, 4H, 4-CH_2, 7-CH_2), 3.10 (s, 3H, 3-OCH_3), 3.88 (s, 3H, Ph-OCH_3), 5.80 (s, 1H, CH), 7. 08–7.23 (m, 2H, Ph). Anal. Calcd for $C_{16}H_{17}ClFNO_3$: C, 58.99; H, 5.26; N, 4.30. Found: C, 58.72; H, 5.50; N, 3.98.

2.4.10. Data for D_{10}

Yield, 78%; yellow oil. ^{1}H NMR (400 MHz, $CDCl_3$): δ = 1.73–1.85 (m, 4H, 5-CH_2, 6-CH_2), 2.31–2.32 (m, 4H, 4-CH_2, 7-CH_2), 3.74 (q, J = 6.4 Hz, 2H, OCH_2CHCH$_2$), 5.02–5.16 (m, 4H, OCH_2CHCH_2, OCH_2Ph), 5.66–5.73 (m, 1H, OCH_2CHCH_2), 5.81 (s, 1H, CH), 7.08–7.45 (m,6H, Ph). Anal. Calcd for $C_{24}H_{22}Cl_2FNO_3$: C, 62.35; H, 4.80; N, 3.03. Found: C, 62.33; H, 5.67; N, 18.17.

2.4.11. Data for D_{11}

Yield, 75%; yellow oil; ^{1}H NMR (400 MHz, $CDCl_3$): δ = 1.73–1.85 (m, 4H), 2.30–2.35 (m, 4H), 3.79–3.96 (m, 2H), 4.57–4.59 (m, 2H), 5.17–5.47 (m, 4H), 5.73 (s, 2H), 5.74–5.81 (m, 1H), 5.99–6.07 (m, 1H), 6.85 (s, 1H), 7.49 (m, 2H). Anal. Calcd for $C_{20}H_{21}ClFNO_3$: C, 63.58; H, 5.60; N, 3.71. Found: C, 63.42; H, 5.58; N, 3.59.

2.4.12. Data for D_{12}

Yield, 76%; yellow oil. ^{1}H NMR (400 MHz, $CDCl_3$): δ = 1.21–1.46 (m, 3H, OCH_2CH_3), 1.73–1.83 (m, 4H, 5-CH_2, 6-CH_2), 2.31–2.34 (m, 4H, 4-CH_2, 7-CH_2), 3.78–3.86 (m, 2H, OCH_2CH_3), 4.02–4.11 (m, 2H, OCH_2CHCH$_2$), 5.10–5.19 (m, 2H, OCH_2CHCH_2), 5.75–5.80 (m, 2H, OCH_2CHCH_2, CH), 7.01–7.22 (m, 2H, Ph). Anal. Calcd for $C_{19}H_{21}ClFNO_3$: C, 62.38; H, 5.79; N, 3.83. Found: C, 62.20; H, 5.73; N, 3.61.

2.5. Herbicidal activities

The herbicidal activities of 29 newly synthesized compounds against *Echinochloa crusgalli* (EC), *Digiatra sanguinalis* (DS), *Setaria viridis* (SV), *Brassica juncea* (BJ), *Amaranthus retroflexus* (AR), *Chenopodium album* (CA) and *Eclipta Prostrata* (EP) were evaluated according to the standard protocol as described previously.[14] All test compounds were formulated as a 150 g/L emulsified concentrates by using DMF as solvent and TW-80 as emulsification reagent. The concentrates were diluted with water to the required concentration and applied to pot-grown plants in a greenhouse. The soil used was a clay soil, pH 6.5, 1.6% organic matter, 37.3% clay particles, and CEC 12.1 mol/kg. The rate of application (g.ai/ha) was calculated by the total amount of active ingredient in the formulation divided by the surface area of the pot. Plastic pots with a diameter of 9.5 cm were filled with soil to a depth of 8 cm. Approximately 20 seeds of *E. crusgalli*, *D. sanguinalis*, *S. viridis*, *B. juncea*, *A. retroflexus*, *C. album* and *E. Prostrata* were sown in the soil at the depth of 1–3 cm and grown at 15–30 °C in a greenhouse. The diluted formulation solutions were applied for post-emergence treatment, dicotyledon weeds were treated at the 2-leaf stage and monocotyledon weeds were treated at the 1-leaf stage, respectively. The post-emergence application rates were 150 g.ai/ha. Untreated seedlings were used as the control group and the solvent (DMF) treated seedlings were used as the solvent control group. Herbicidal activity was evaluated visually after 15 days post treatment. The results of herbicidal activities were summarized in Table 2.

2.6. CoMFA anlysis

The 3D structures of all the compounds were built by SYBYL 7.3/Sketch,[18] and then optimized using MMFF94 force field,[19] by Powell method with energy termination of 0.005 kcal/mol, and a maximum of 1000 iterations. Then, the Gasteiger–Hückel charges were added. Pharmacophore-based molecule alignment method was applied to superimpose all the compounds by using GALAHAD in SYBYL 7.3. The steric and electrostatic field energies for CoMFA were calculated using the SYBYL default parameters: 2.0Å grid points spacing, a sp^3 carbon probe atom with +1 charge and a *van der Waals* radius of 1.52Å, and column filtering of 2.0 kcal/mol. The CoMFA descriptors were used as independent variables, and pk_i values were used as dependent variables in partial least-squares (PLS) regression analyses to derive 3D-QSAR models. Leave-one-out (LOO) cross-validated PLS analyses were performed to determine the optimal number of components to be used in the final QSAR models and to check the predictive ability of the

Table 2
Post-emergency herbicidal activity of compounds **A**–**D** (150 g·ai/ha)

No.	EC [a]	DS	SV	BJ	AR	CA	EP
A_1	+[b]	+	+	+	+++	–	+
A_2	–	–	–	–	–	–	–
A_3	–	–	–	+	+++	+	++
B_1	–	–	–	–	–	–	–
B_2	–	–	–	–	–	–	–
B_3	–	–	–	–	–	–	–
B_4	–	–	–	–	–	–	–
B_5	–	–	–	–	–	–	–
B_6	–	–	–	–	–	–	–
B_7	–	–	–	–	–	–	–
C_1	–	–	+	++	+++	++	++
C_2	–	–	–	–	–	–	–
C_3	–	–	–	–	+	+	+
C_4	++	++	++	+	++	+++	+
C_5	–	–	–	–	++	–	–
C_6	++	++	++	++	++	+++	+++
C_7	++	++	++	++	+++	+++	+++
D_1	–	+	–	–	+	+	+
D_2	–	+	–	+	++	+	+
D_3	–	–	–	+	+	+	+
D_4	–	–	–	+	+	+	+
D_5	–	–	–	+	++	++	+
D_6	–	–	–	–	++	+	+
D_7	+	+	–	–	+	+	+
D_8	+	–	–	+	+	+	+
D_9	+	+	+	+	++	++	+
D_{10}	–	+	–	–	++	–	+
D_{11}	+	++	++	+++	+++	++	++
D_{12}	+	+	+	+	+++	+++	+++
Sulfentrazone	–	–	++	+++	+++	+++	+++

[a] EC for *E. crusgalli*, DS for *D. sanguinalis*, SV for *S. viridis*, BJ for *B. juncea*, AR for *A. retroflexus*, CA for *C. album* and EP for *E. Prostrata*.
[b] Rating system for the growth inhibition percentage: +++, 100%; ++, >80%; +, 50–80%; –, <50%.

models. To visualize the 3D-QSAR results in term of field contributions, isocontour maps were generated using the field type 'stdev * coeff' and the contour levels were set to default values. In CoMFA, compounds **24** and **5** were selected randomly as the training set and the test set, respectively.

2.7. X-ray diffraction

Colorless crystal of $\mathbf{C}_4$ (0.30 × 0.20 × 0.20 mm) was mounted on a thin quartz fiber for X-ray diffraction data collection. Initial cell constants were indexed by three separated 'matrix' runs using 3151 reflections. Intensity data sets were collected on a Bruker SMART APEX CCD diffractometer with graphite monochromated Mo Kα radiation (λ = 0.71073 Å) in the $2.10 \leqslant \theta_{max} \leqslant 27.25°$ range.

Table 3
Crystal data and structural refinement parameters for $\mathbf{B}_1$ and $\mathbf{C}_4$

	$\mathbf{B}_1$	$\mathbf{C}_4$
Empirical formula	$C_{19}H_{22}ClFNO_3$	$C_{16}H_{17}ClFNO_2$
Formula weight	366.83	309.76
Crystal system	Monoclinic	Triclinic
Space group	$P2_1/c$	P-1
Unit cell dimensions		
a (Å)	12.1284(15)	8.7953(10)
b (Å)	11.1700(14)	8.9495(11)
c (Å)	13.7126(17)	10.4144(12)
α (°)	90	103.523(2)
β (°)	95.752(2)	103.998(2)
γ (°)	90	99.048(2)
Volume (Å^3)	1848.4(4)	753.23(15)
Z	4	2
Calcd density (Mg/m^3)	1.318	1.366
F(0 0 0)	772	324
Crystal size (mm)	0.30 × 0.20 × 0.20	0.20 × 0.20 × 0.15
θ range (°)	1.69–27.50	2.10–27.25
Reflections collected	17,103	7207
Independent reflections	4219	3324
Number of parameters	227	211
Goof	1.045	1.096
Final R indices [$I > 2\sigma(I)$]	R_1 = 0.0595, wR_2 = 0.1586	R_1 = 0.0496, wR_2 = 0.1373
R indices (all data)	R_1 = 0.0710, wR_2 = 0.1684	R_1 = 0.0624, wR_2 = 0.1529
Max. diff. peak and hole (eÅ^{-3})	0.423, −0.326	0.168, −0.246

A total number of 7207 reflections were measured of which 3324 reflections were independent with R_{int} = 0.0619. The data sets were corrected for Lorentz and polarization effects and for absorption (T_{min} = 0.924; T_{max} = 0.948). The structure was solved by direct methods using *SHELXS*-97[20] and refined on F^2 by full-matrix least-squares techniques with *SHELXL* package program.[21] All the non-hydrogen atoms were refined anisotropically and all the hydrogen atoms were positioned at there ideal positions. In the refinement, the C2–C5 atoms on the cyclohexyl group were disordered over two sites. They are refined by using these commands 'SADI' and 'ISOR'. The final occupancies were 0.74:0.26 for the major and minor components, respectively. Similarly, data sets of colorless crystal of B1 were collected in the $1.69 \leqslant \theta_{max} \leqslant 27.50°$ range. A total number of 17103 reflections were measured of which 4219 reflections were independent with R_{int} = 0.0212. The data sets were corrected for Lorentz and polarization effects and for absorption (T_{min} = 0.923; T_{max} = 0.955). The refinement of $\mathbf{B}_1$ was in a similar way to that of complex $\mathbf{C}_4$. Relevant crystal data, collection parameters and refinement results can be found in Table 3.

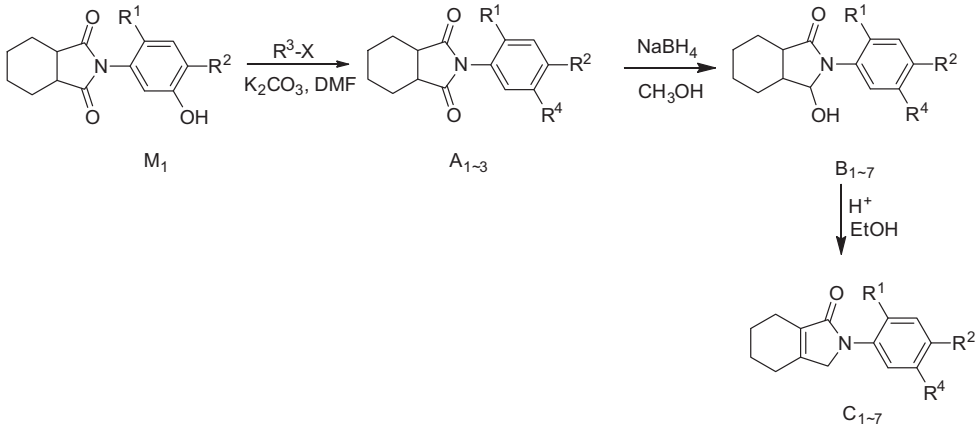

Scheme 1. Synthetic route for the target compounds **A**–**C**.

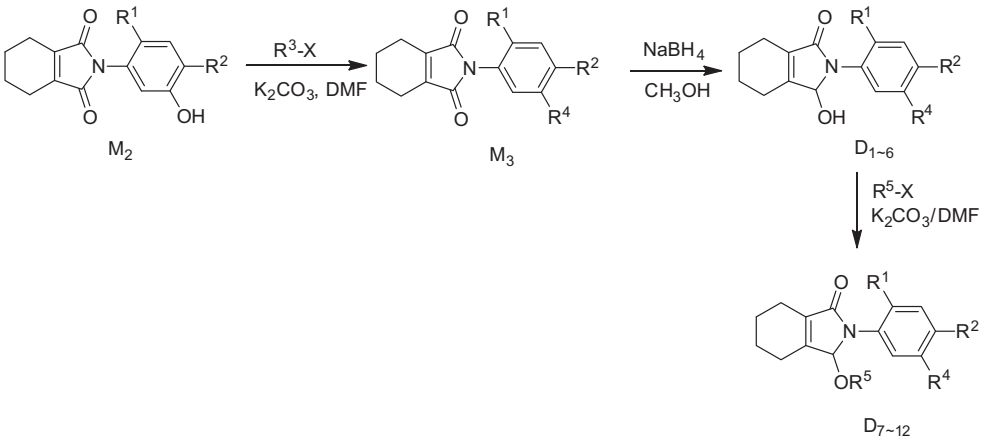

Scheme 2. Synthetic route for the target compound **D**.

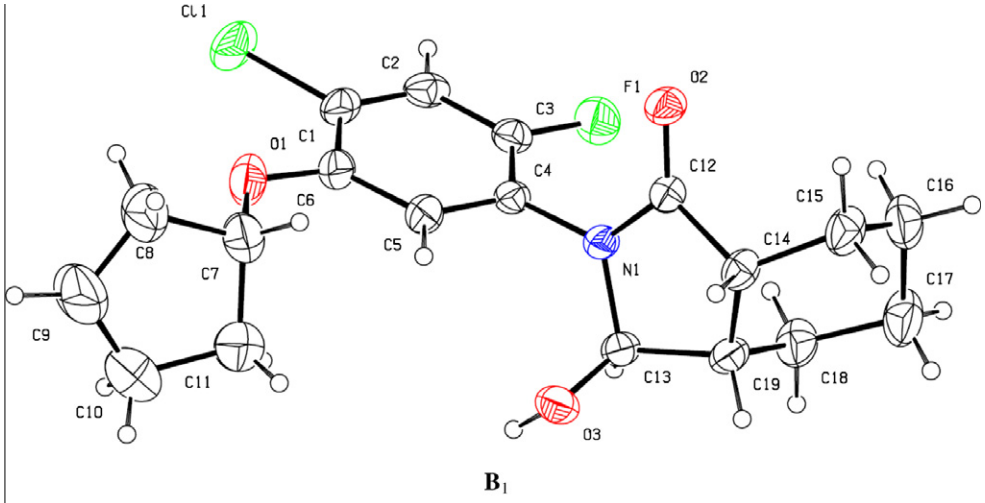

B_1

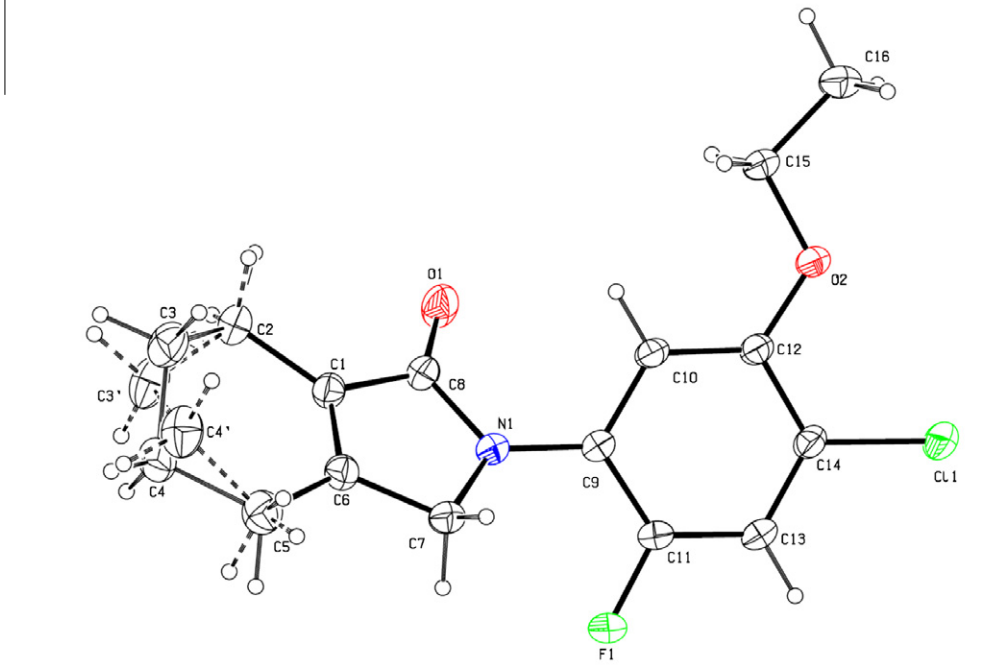

C_4

Figure 3. Crystal structures of B_1 and C_4.

3. Results and discussion

3.1. Synthesis of the title compounds

As shown in Scheme 1, the target compounds **A**–**C** were prepared by using 2-(5-hydroxy-2,4-disubstitutedphenyl)hexahydroisoindole-1,3-dione ($\mathbf{M}_1$) as starting material. At the presence of potassium carbonate, alkylation of $\mathbf{M}_1$ with various alkyl halide afforded the desired compounds $\mathbf{A}_{1-3}$ in yields of 75–88%. Then, treatment of compound **A** with methanol solution of $NaBH_4$ resulted in compounds $\mathbf{B}_{1-7}$ in yields of 68–95%. In ethanol solution of concentrated hydrochloric acid, compound **B** underwent dehydration smoothly to afford the desired compounds $\mathbf{C}_{1-7}$ in yields of 70–85%.

As shown in Scheme 2, the target compound **D** was synthesized by using 2-(5-hydroxy-2,4-disubstitutedphenyl)-4,5,6,7-tetrahydro-isoindole-1,3-dione ($\mathbf{M}_2$) as starting material. Firstly, $\mathbf{M}_2$ took place alkylation reaction with various alkyl halide at the presence of potassium carbonate to provide intermediate $\mathbf{M}_3$ in excellent yields. Then, one of the carbonyl group was reduced to hydroxyl group with sodium borohydride to afford compound **D**, some of which reacted with various alkyl halide at the presence of potassium carbonate to obtain the hydroxyl-protected compound **D**.

The structures of all intermediates and title compounds were confirmed by elemental analyses, ^{1}H NMR and MS spectral data. In addition, the crystal structures of compounds $\mathbf{B}_1$ and $\mathbf{C}_4$ were determined by X-ray diffraction analyses as shown in Figure 3. The cyclohexane ring of compound $\mathbf{B}_1$ takes chair conformation, the crystal packing is stabilized by three intermolecular hydrogen-bonding [C(14)–H(14)···O(3), C(2)–H(2)···O(2), O(3)–H(3)···O(2)] interactions. In addition, the dihedral angel between the benzene ring and the isoindolone ring of compound $\mathbf{C}_4$ is 40.2°, while two carbon atoms [C(3) and C(4)] of the cyclohexene moiety are disordered.

3.2. PPO-inhibiting activity and CoMFA analysis

The k_i values against human PPO of the newly synthesized 29 compounds were listed in Table 1. 4-Chlorophthalimide and sulfentrazone were used as positive control. As shown in Table 1, most of the newly design and synthesized compounds showed higher PPO-inhibiting activity than 4-chlorophthalimide. However, all of compounds **A**, **B** and **D** (except for compounds $\mathbf{D}_2$ and $\mathbf{D}_3$) exhibited lower activity than sulfentrazone. Most interestingly, all of compound **C** (except for compound $\mathbf{C}_2$), the mono-carbonyl analogues of cyclic imides, displayed higher in vitro PPO inhibition activity than sulfentrazone, among which compound $\mathbf{C}_6$ (k_i = 0.095 μM) is 7.6-folds higher active than sulfentrazone (k_i = 0.72 μM). These results confirmed once again that only one of the carbonyl groups of cyclic imides is essential to the PPO inhibition activity.

In order to understand the substituent effects on the PPO inhibition of these compounds, the method of comparative molecular field analysis (CoMFA) was applied to understand the quantitative structure–activity relationships. As listed in Table 4, a predictive CoMFA model was established with the conventional correlation coefficient r^2 = 0.980 and the cross-validated coefficient q^2 = 0.518, the contribution of steric and electrostatic fields are 48.5% and 51.5%, respectively. The observed and calculated activity values for all the compounds are given in Table 1, and the plots of the predicted versus the actual activity values for all the compounds are shown in Figure 4. In Figure 5, the isocontour diagrams of the steric and electrostatic field contributions ("stdev*coeff") obtained from the CoMFA analysis are illustrated together with exemplary ligands. The steric field contour map is plotted in Figure 5A. The green region highlights positions where a bulky group would be favorable for higher PPO inhibition activity. In contrast, yellow indicates positions where a decrease in the bulk of the desired compounds is favored. As shown in Figure 5A, the CoMFA steric contour plots indicated that a big yellow region is located around the group of R^5, while a big green region surrounded the R^4 group. This map means that the R^4 and R^5 substituents should be bulky and small groups, respectively. This steric map explained clearly why compound **C** except for $\mathbf{C}_3$ always displayed higher activity ($6.16 < pk_i < 7.02$) than other compounds. The electrostatic contour plot is shown in Figure 5B. The blue contour defines a region where an increase in the positive charge will result in an increase in the activity, whereas the red contour defines a region of space where increasing electron density is favorable. As shown in Figure 5B, the target compounds bearing an electron-withdrawing group at the position of R^1 and R^4 will display higher activity. For example, compounds containing fluorine atom at position R^1 always displayed higher activity than other compounds, such as compound $\mathbf{C}_2$ (R^1 = H), $\mathbf{C}_5$ (R^1 = Cl), $\mathbf{D}_4$ (R^1 = Cl), and $\mathbf{D}_6$ ($R^1 = OCH_2CH_3$). In addition, the electrostatic contour plot showed that a red region is around the carbonyl group, whereas a blue region is around the R^5 group. This contour map indicated that the more electronegative the oxygen atom of the carbonyl, the higher the activity of inhibitors, which is accordance with our previous DFT-QSAR result[13] that the approximate nucleophilic superdelocalizability of the carbon atom of one of the carbonyl group played an important role in determining the activity of PPO inhibitors. The stronger the ability of the carbonyl group to accept electrons from receptor, the higher the activity of PPO inhibitor.

3.3. Greenhouse herbicidal activities

The post-emergence herbicidal activity of series **A**–**D** were tested in greenhouse at the concentration of 150 g.ai/ha, a

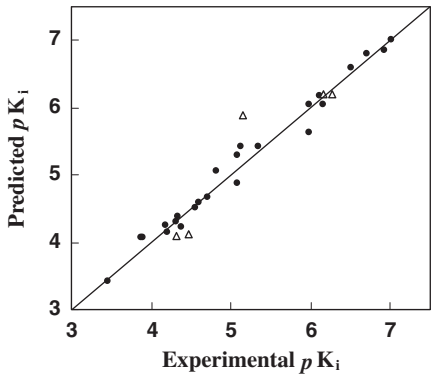

Figure 4. Predicted pk_i (*Y*-axis) are versus experimental pk_i (*X*-axis) values. The dots and the triangle represent training and test compounds, respectively.

Table 4
Statistical results of CoMFA

Method	Cross-validation		Conventional			Contribution	
	q^2	OCN	r^2	F	SEE	Steric	Electrostatic
CoMFA	0.518	5	0.980	175.441	0.168	0.485	0.515

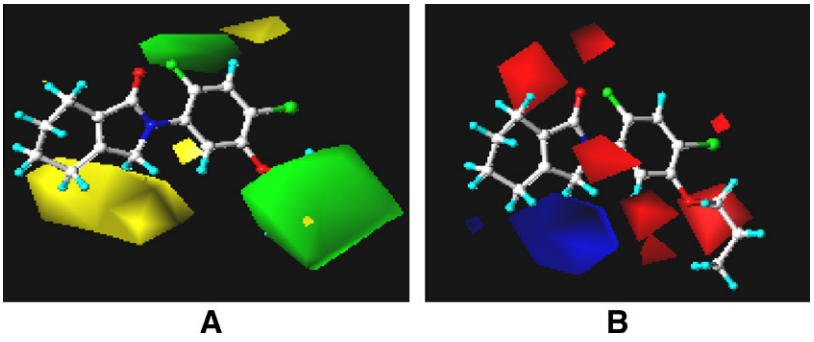

Figure 5. CoMFA contour maps with compound **16** as the reference structure. (A) Steric contours. Scattered green areas are regions where bulky substituents are favorable, yellow areas are unfavorable. (B) Electrostatic contours. The red areas are the regions where negative potential is favorable for the activity, blue areas are unfavorable.

triazolinone-type commercial product, sulfentrazone, was selected as a positive control. As shown in Table 3, some of compounds ($\mathbf{C}_1$, $\mathbf{C}_4$, $\mathbf{C}_6$, $\mathbf{C}_7$, $\mathbf{D}_{11}$ and $\mathbf{D}_{12}$) were found to display promising and broad spectrum herbicidal activities. Most interestingly, compounds $\mathbf{C}_6$ and $\mathbf{C}_7$ displayed over 80% inhibiting activities against all seven tested weeds. However, sulfentrazone did not show significant herbicidal activity against monocot weeds, such as *E. crusgalli* and *D. sanguinalis.* These results showed that these compounds have the potential for further test with crop selectivity and herbicidal spectrum.

4. Conclusions

In summary, based on previous DFT-QSAR results, a series of mono-carbonyl analogues of cyclic imides, *N*-phenyl pyrrolidin-2-ones and *N*-phenyl-1*H*-pyrrol-2-ones, were designed and synthesized as potential PPO inhibitors. The in vitro test results indicated that most of the newly synthesized compounds have good or excellent PPO inhibition activity. Additionally, a 3D-QSAR analysis was performed with the method of CoMFA to explore the comprehensive structure–activity relationships and a statistically reliable model with good predictive power ($r^2 = 0.980$, $q^2 = 0.518$) was achieved on the basis of pharmacophore-based molecule alignment. The CoMFA analysis indicated that a bulkier substitutent R^4 and a smaller substitutent R^5 is favorable for high PPO inhibition, meanwhile, an electron-withdrawing substitutent R^1 is priority for inhibitors with higher potency. This observation was confirmed by the in vitro PPO inhibition results of compounds **C**, which showed much higher activity than other compounds. Moreover, our further greenhouse assay against seven weeds leaded to two most promising candidates, namely, 2-(4-chloro-2-fluoro-5-propoxy-phenyl)-2,3,4,5,6,7-hexahydro-isoindol-1-one ($\mathbf{C}_6$, $k_i = 0.095$ μM) and 2-(5-allyloxy-4-chloro-2-fluorophenyl)-2,3,4,5,6,7-hexahydro-isoindol-1-one ($\mathbf{C}_7$, $k_i = 0.12$ μM), which exhibited high PPO inhibition and broad spectrum herbicidal activity at the concentration of 150 g.ai/ha. These results confirmed once again the reliability of previous DFT-QSAR study, which showed that only one of the carbonyl groups of cyclic imides is essential to the PPO inhibition activity. The further crop selectivity and field trial of these two compounds are under the way.

Acknowledgments

We thank Dr. Jie Chen for the greenhouse test of biological activities. We also thank the financial support from the National Basic Research Program of China (No. 2010CB126103), the NSFC (Nos. 20925206, 20932005 and 21002038) and the PCSIRT (No. IRT0953).

References and notes

1. Corradi, H. R.; Corrigall, A. V.; Boix, E.; Mohan, C. G.; Sturrock, E. D.; Meissner, P. N.; Acharya, K. R. *J. Bio. Chem.* **2006**, *281*, 38625.
2. Koch, M.; Breithaupt, C.; Kiefersauer, R.; Freigang, J.; Huber, R.; Messerschmidt, A. *EMBO J.* **2004**, *23*, 1720.
3. Zhao, Q. Q.; Liu, S. H.; Li, Y. H.; Wang, Q. M. *J. Agric. Food Chem.* **2009**, *57*, 2849.
4. Theodoridis, G.; Princetons, N. J. U.S. Patent 4,818,275, 1989.
5. Hiraki, M.; Ohki, S.; Sato, Y.; Jablonkai, I.; Boger, P.; Wakabayashi, K. *Pestic. Biochem. Phys.* **2001**, *70*, 159.
6. Theodoridis G. U.S. Patent 5,798,316, 1989.
7. Hirai, K.; Futikami, T.; Murata, A.; Hirose, H. U.S. Patent 4,818,272, 1989.
8. Liu, Y. X.; Cui, Z. P.; Liu, B.; Cai, B. L.; Li, Y. H.; Wang, Q. M. *J. Agric. Food Chem.* **2010**, *58*, 2685.
9. Nagano, E.; Hashimoto, S.; Yoshida, R.; Matsumoto, H.; Oshio, H.; Kamoshita, k. EP 61741, 1982.
10. Theodoridis, G.; Poss, K. M.; Hotzman, F. W. In *Synthesis and Chemistry of Agrochemicals IV*; American Chemical Society: Washington, DC, 1995.
11. Theodoridis, G.; Bahr, J. T.; Davidson, B. L.; Hart, S. E.; Hotzman, F. W.; Poss, K. M.; Tutt, S. F. E. In *Synthesis and Chemistry of Agrochemicals IV*; American Chemical Society: Washington, DC, 1995.
12. Wakabayashi, K.; Böger, P. *Z. Naturforsch. C.* **1995**, *50*, 591.
13. Wan, J.; Zhang, L.; Yang, G. F.; Zhan, C. G. *J. Chem. Inf. Comp. Sci.* **2004**, *44*, 2099.
14. Jiang, L. L.; Tan, Y.; Zhu, X. L.; Wang, Z. F.; Zuo, Y.; Chen, Q.; Xi, Z.; Yang, G. F. *J. Agric. Food Chem.* **2010**, *58*, 2643.
15. Luo, Y. P.; Jiang, L. L.; Wang, G. D.; Chen, Q.; Yang, G. F. *J. Agric. Food Chem.* **2008**, *56*, 2118.
16. Huang, M. Z.; Huang, K. L.; Ren, Y. G.; Lei, M. X.; Huang, L.; Hou, Z. K.; Liu, A. P.; Ou, X. M. *J. Agric. Food Chem.* **2005**, *53*, 7908.
17. Huang, M. Z.; Cheng, P.; Huang, K. L.; Ren, Y. G.; Lei, M. X.; Ma, Y. G.; Xu, M. C. *Chin. J. Org. Chem.* **2005**, *25*, 949.
18. SYBYL 7.3. S. Hanely Road, St. Louis, MO 63144, USA.
19. Halgren, T. *J. Am. Chem. Soc.* **1990**, *112*, 4710.
20. Sheldrick, G. M. SHELXTL (version 5.0); University of GÖttingen: GÖttingen, Germany, 2001.
21. SMART V5.628, SAINT V6.45, and SADABS; Bruker AXS Inc: Madison, WI, 2001.